

A Unified Approach to Phase Equilibria in Multi-component Polymer Systems with Effective Chemical Potential

Wei-Ling Huang, Yu-Chen Zhang, and Yi-Xin Liu*

State Key Laboratory of Molecule Engineering of Polymers, Department of Macromolecular Science, Fudan University, Shanghai 200433, China

 Electronic Supplementary Information

Abstract Multi-component polymer systems exhibit exceptional versatility and structural diversity, making them indispensable in the polymer industry as well as in advanced and high performance applications. However, constructing accurate phase diagrams for these systems remains challenging due to inhomogeneous structures arising from the introduction of block copolymer components. Here, we present a unified and model-agnostic framework for computing phase equilibria in multi-component polymeric systems based on the concept of “effective chemical potential”. This approach directly connects key thermodynamic variables in the canonical ensemble to other ensembles, unifying phase coexistence determination without requiring the reformulation of self-consistent field theory (SCFT) calculations across different ensembles. By decoupling phase equilibrium determination from specific ensemble formulations, our approach enables the reuse of existing SCFT solvers. Moreover, it provides a useful framework to develop highly efficient phase equilibrium solvers for multi-component polymer systems.

Keywords Polymer blends; Chemical potential; Phase equilibrium; Block copolymers

Citation: Huang, W. L.; Zhang, Y. C.; Liu, Y. X. A unified approach to phase equilibria in multi-component polymer systems with effective chemical potential. *Chinese J. Polym. Sci.* <https://doi.org/10.1007/s10118-025-3369-8>

INTRODUCTION

Multi-component polymeric systems have attracted significant attention due to their remarkable tunability and structural diversity, which far exceed those of neat polymers.^[1–4] By incorporating multiple components, these systems enable the formation of novel stable and metastable phases, as well as regions of multiphase coexistence.^[5–8] These phase structures find applications in diverse fields, including biodegradable materials,^[9,10] thermoplastic elastomers,^[11–13] semiconductor film formation,^[14,15] optoelectronics,^[16–18] and lithography.^[19,20] As industries^[21,22] increasingly rely on multi-component systems for high-performance materials, understanding and controlling their phase behavior is critical. For instance, precise control of phase behavior in semiconductor films can significantly enhance material performance and processing efficiency.^[23–26]

Tailoring compositions to stabilize desired phases remains a key challenge. While neat block copolymers often face synthetic constraints on chain architectures, multi-component systems allow for more intricate structural arrangements through compositional tuning.^[27,28] For example, adding homopolymers to a diblock copolymer system induces complex arrangements of spherical domains such as C14 and C15 phases,^[29–31] which are difficult to stabilize in neat diblock

copolymers. Furthermore, multiblock copolymer blends expand the possibilities for generating sophisticated phases, including binary mesocrystals and hybrid morphologies, thus providing an ideal platform for engineering of functional materials.^[32–34]

Accurate phase diagrams are crucial for guiding composition selection to achieve desired phases.^[35] However, constructing these diagrams involves managing complex thermodynamic variables, such as concentrations, chemical potentials, and free energies, which pose significant challenges in high-dimensional parameter spaces.^[36] Identifying stability windows requires expertise and significant effort in both theoretical^[37–39] and experimental studies.^[27,28]

Canonical ensemble (CE)-based methods, such as the double-tangent construction^[35] are widely recognized for their simplicity and stability. However, such an approach often requires extensive computational resources for free energy calculations, making it suitable for demonstration purposes only. In a more recent development, Matsen^[40] reformulated the self-consistent field theory (SCFT) in the grand canonical ensemble (GCE) instead of the CE used by the original formulation. In the GCE, the phase coexistence can be trivially determined by simply equating the grand canonical free energies between candidate phases. However, as the control variables in the GCE are chemical potentials which relate to the composition in a non-intuitive way, it suffers from stability issues due to difficulties in selecting suitable initial values for chemical

* Corresponding author, E-mail: lyx@fudan.edu.cn

Received February 24, 2025; Accepted May 2, 2025; Published online June 30, 2025

potentials. To address this, Matsen^[41] later proposed a hybrid CE-GCE method, where initial values are first computed in CE and then fed into GCE calculations. Despite reducing initialization challenges, this method discards data gathered from CE calculations, leading to significant waste of computational resources.

More recently, Mester, Lynd and Fredrickson^[42] developed a new method for computing phase diagrams of binary polymer blends based on the Gibbs ensemble (GE) SCFT calculations. They considered the phase equilibrium problem as an optimization problem in Gibbs ensemble, which is then solved by a conjugate gradient solver. It is demonstrated that the GE method enjoys the universally convergent property inherited from the conjugate gradient solver and converges even when the initial values are far from the actual solution. However, one drawback of the Gibbs approach is that every time the architecture of either component in polymer blends changes, the full set of equations has to be re-derived and the associated numerical algorithm should be reimplemented. Unfortunately, the existing canonical SCFT implementations cannot be reused due to the built-in entanglement of SCFT calculation and phase coexistence determination logic in the GE approach.

For ternary and higher-component systems, the complexity of phase equilibrium calculations increases substantially. In CE, free energy landscapes expand from one-dimensional curves to multidimensional hypersurfaces, requiring the identification of a common tangent hyperplane across multiple hypersurfaces to determine phase coexistence. This geometrical complexity is further exacerbated in GCE, where phase coexistence is determined by identifying a common intersection among multiple free energy curves. These tasks require extensive computational resources due to the high-dimensional nature of the parameter space and necessitate robust optimization algorithms to achieve accurate results.

Several methods have been proposed to address these challenges. For example, Park, Bates and Dorfman^[43] developed a GCE-based approach for ternary systems by fixing the chemical potential of one component at zero and systematically varying the remaining two chemical potentials to locate phase coexistence points. Although doable in principle, this method is computationally intensive, as the parameter space for chemical potentials ranges from negative to positive infinity. Moreover, the initialization of appropriate starting values remains a significant challenge, often leading to convergence instability. As another example, Xie and Shi^[44] introduced a semi-grand canonical ensemble (semi-GCE) approach for the AB/C/D ternary polymer blend, transforming three chemical potential variables into two chemical potentials variables and one volume fraction variable. This transformation makes it more manageable compared to using unbounded chemical potential variables. However, both the GCE and semi-GCE approaches are heavily coupled with the underlying SCFT calculations required for free energy calculations. Adapting SCFT to operate within these ensembles requires substantial reformulation, thereby limiting the scalability of these methods. Furthermore, consistently extending these frameworks to systems with an arbitrary number of components is rarely explored.

Despite the progress made by various methods, current approaches for determining phase equilibria in polymer blend systems often exhibit fragmentation in their treatment of key thermodynamic variables like free energy, volume fractions, and chemical potentials. For instance, Matsen's formulation embeds chemical potentials within SCFT in a tightly coupled manner,^[41] which complicates both conceptual understanding and extension to multi-component systems. Similarly, phase equilibrium methods developed by Dorfman^[43] and Shi^[44] for ternary blends are also deeply coupled with SCFT, restricting their applicability to arbitrary component systems.

In this study, we present a unified approach for determining phase equilibrium in multi-component systems by leveraging the concept of "effective chemical potential". Our approach directly connects key thermodynamic variables in CE to other ensembles, such as GCE and GE, thereby allowing these variables to be calculated exclusively in CE. Consequently, subsequent phase equilibrium calculations can be carried out in any ensemble, which unifies the determination of phase equilibrium across all previously mentioned approaches. Our approach not only provides a consistent framework for developing various phase coexistence solvers through a concise and generalized formulation, but also enhances compatibility with existing theoretical frameworks, such as Flory-Huggins theory and various phase field-based simulations. It allows for applications to multi-component systems of arbitrary complexity. Furthermore, by decoupling the phase equilibrium calculation process from specific ensemble formulations used in free energy calculations, our approach allows for the exploration of novel free energy models.

GENERAL FORMULATION

In this section, we introduce a general formulation of the coexistence condition for polymer blends with $n_c \geq 2$ components and $n_\varphi \geq 2$ phases. The chemical potential is defined as the first-order derivative of the free energy in the *canonical ensemble* (CE) with respect to n_p , being the number of particles of component $p \in \{1, 2, \dots, n_c\}$,

$$\mu_p = \left(\frac{\partial F}{\partial n_p} \right)_{l_p} \quad (1)$$

where $l_p = \{n_i \mid i = 1, 2, \dots, n_c, i \neq p\}$ is a set of number variables for components other than p .

At the equilibrium state, the chemical potential of each component p , μ_p^φ , is equal in each coexisting phases $\varphi \in \{\alpha, \beta, \dots, \zeta\}$, $\mu_p^\alpha = \mu_p^\beta = \dots = \mu_p^\zeta$. It follows that subtracting the chemical potentials of any two components p and q ($p \neq q$) between any pair of coexisting phases remains equal, $\mu_p^\alpha - \mu_q^\alpha = \mu_p^\beta - \mu_q^\beta = \dots = \mu_p^\zeta - \mu_q^\zeta$. Based on this relation, it is natural to define an "effective chemical potential" for component p by choosing the chemical potential of a reference component (*e.g.*, component r),

$$\tilde{\mu}_p \equiv \mu_p - \mu_r \quad (2)$$

The physical meaning of this quantity will be clarified later. Clearly, the effective chemical potential of the reference component itself is 0, *i.e.*, $\tilde{\mu}_r = 0$. Without loss of generality, in

practice we can choose the last component as the reference such that $r = n_c$.

In practice, it can be more convenient to use volume fractions instead of moles as independent variables. The free energy of the system as a function of volume fractions is given by, $\tilde{F}(\phi_1, \phi_2, \dots, \phi_{n_c}) = \frac{1}{n}F(n_1, n_2, \dots, n_{n_c})$, where ϕ_p is the volume fraction of the p -th component and $n = \sum_{p=1}^{n_c} n_p$ is the total number of moles of all components in the system. Note that \tilde{F} is intentionally written as a function of all n_c volume fractions, despite the fact that only $n_c - 1$ of them are independent due to the mass conservation constraint $\sum_{p=1}^{n_c} \phi_p = 1$.

Combining Eq. (1) with the above relations $\tilde{F}(\phi_1, \phi_2, \dots, \phi_{n_c}) = \frac{1}{n}F(n_1, n_2, \dots, n_{n_c})$ and utilizing $\frac{\partial \phi_p}{\partial n_p} = \frac{1 - \phi_p}{n}$ and $\frac{\partial \phi_q}{\partial n_p} = -\frac{\phi_q}{n}$

for $p \neq q$, the chemical potential of component p can also be expressed as,^[45] $\mu_p = \tilde{F} + \left(\frac{\partial \tilde{F}}{\partial \phi_p}\right)_{\tilde{l}_p} - \sum_{q=1}^{n_c} \left(\frac{\partial \tilde{F}}{\partial \phi_q}\right)_{\tilde{l}_q} \phi_q$, where

$\tilde{l}_p = \{\phi_i \mid i = 1, 2, \dots, n_c, i \neq p\}$ is a set of volume fraction variables of components other than component p similar to l_p . For clarity, it is assumed that all segments of different kinds of monomers have identical volume. And the derivatives are taken without considering the mass constraint. In other words, all n_c volume fractions are treated as if they are "independent".

By substituting the expression for μ_p from the previous formula into the definition of the effective chemical potentials $\tilde{\mu}_p$ in Eq. (2), we arrive at another expression for the effective chemical potential,

$$\tilde{\mu}_p = \left(\frac{\partial \tilde{F}}{\partial \phi_p}\right)_{\tilde{l}_p} - \left(\frac{\partial \tilde{F}}{\partial \phi_r}\right)_{\tilde{l}_r} \quad (3)$$

It is helpful to introduce the following quantity,

$$Y_p \equiv \left(\frac{\partial \tilde{F}}{\partial \phi_p}\right)_{\tilde{l}_p} \quad (4)$$

so that we can express Eq. (3) in a more concise form: $\tilde{\mu}_p = Y_p - Y_r$. Y_p is the essential quantity to compute as it simplifies the computation of the chemical potential.

Besides serving as a convenient computing vehicle for the effective chemical potential, Eq. (3) also provides a way to understand its physical essence. To illustrate this, we first rewrite the right-hand side of Eq. (3),

$$\left(\frac{\partial \tilde{F}}{\partial \phi_p}\right)_{\tilde{l}_p} - \left(\frac{\partial \tilde{F}}{\partial \phi_r}\right)_{\tilde{l}_r} = \left(\frac{\partial \tilde{F}}{\partial \phi_p}\right)_{\tilde{l}_p} \frac{\partial \phi_p}{\partial \phi_p} + \left(\frac{\partial \tilde{F}}{\partial \phi_r}\right)_{\tilde{l}_r} \frac{\partial \phi_r}{\partial \phi_p} \quad (5)$$

which is equivalent to the partial derivative of \tilde{F} with respect to ϕ_p , allowing both ϕ_p and ϕ_r to vary. Consequently,

$$\tilde{\mu}_p = \left(\frac{\partial \tilde{F}}{\partial \phi_p}\right)_{\tilde{j}_p} \quad (6)$$

where $\tilde{j}_p = \{\phi_i \mid i = 1, 2, \dots, n_c, i \neq p, r\}$ is a set of volume fraction variables of components other than p and r . Clearly, Eq. (6) has a form similar to Eq. (1). Thus, the effective chemical potential shares a similar meaning with the bare chemical potential: it

is the "chemical potential" by taking the $n_c - 1$ volume fractions (excluding ϕ_r) as independent variables. From a geometrical point of view, $\tilde{\mu}_p$ is the slope of the tangent hyperplane of the free-energy hyper-surface along the direction of the ϕ_p coordinate.

Remarkably, in terms of the effective chemical potentials, it can be shown that the equilibrium coexistence condition within CE follows a similar set of equations to the bare chemical potential formulation,^[35]

$$\begin{cases} \tilde{\mu}_p^\alpha = \tilde{\mu}_p^\beta = \dots = \tilde{\mu}_p^\zeta = \tilde{\mu}_p \\ \tilde{F}^{\alpha_1} - \tilde{F}^{\alpha_2} = \sum_{p=1, p \neq r}^{n_c} (\phi_p^{\alpha_1} - \phi_p^{\alpha_2}) \tilde{\mu}_p \end{cases} \quad (7)$$

In the above equations, it is understood that each $p \in \{i \mid i = 1, 2, \dots, n_c, i \neq r\}$ and each pair of $(\alpha_1, \alpha_2) \in \{(i, j) \mid i, j = \alpha, \beta, \dots, \zeta, i \neq j\}$ should be applied to Eq. (7). As a consequence, the above equilibrium conditions can only be satisfied by a common tangent hyperplane to $\tilde{F}^{\alpha_1}, \tilde{F}^{\alpha_2}$ surfaces in the $n_c - 1$ dimensional space. If the analytical form of $\tilde{F}(\phi)$ is known, the most straightforward way to calculate the two-phase equilibria is treating the equilibrium conditions as a set of nonlinear equations and solving them with a nonlinear solver, which is equivalent to construct the common tangent hyperplane to the free energy density surfaces. In general, the solution of a two-phase equilibria problem is an $n_c - 2$ dimensional surface embedded in the hyperplane, $\sum_{i=1}^{n_c} \phi_p = 1$, of an n_c dimensional space. In particular, they are a pair of points and a curve for binary and ternary systems, respectively. A typical common tangent curve for a binary system is illustrated in Fig. 1.

If necessary, it is also straightforward to convert the CE free energy to GCE free energy through a Legendre transform,^[46]

$$\tilde{F}_g = \tilde{F} - \sum_{p=1, p \neq r}^{n_c} \tilde{\mu}_p \phi_p \quad (8)$$

Here, $\tilde{\mu}_p$ is the chemical potential corresponding to the volume fractions at ϕ_p . Consequently, the equilibrium condition is replaced by a much simpler form,

$$\tilde{F}_g^\alpha = \tilde{F}_g^\beta = \dots = \tilde{F}_g^\zeta \quad (9)$$

In practice, the phase equilibria can be calculated by finding the intersection of \tilde{F}_g surfaces for all phases. Particularly, for the two-phase coexistence with a binary system, there is only one free variable. Thus a root-finding algorithm can be readily applied to find the intersection. The resulting solution, $\tilde{\mu}_p$ is then converted to the desired volume fractions ϕ_p , through inverting the mapping $\tilde{\mu}_p(\phi_p)$. Based on the above formulation, we would like to point out that the GCE free energy \tilde{F}_g can be computed from the CE free energy \tilde{F} without performing any additional computations in GCE. For more detailed derivations for the two-component and three-component systems can be found in the Section 1 of the electronic supplementary information (ESI).

The CE free energy can also be converted to the Gibbs ensemble free energy,

$$G = v^\alpha \tilde{F}^\alpha + v^\beta \tilde{F}^\beta \quad (10)$$

which is optimized to obtain phase equilibrium as below,

$$\begin{aligned} \min_{\phi_p^a, \phi_p^b} G(\phi_p^a, \phi_p^b) \\ \text{s.t. } 0 < \phi_p^a < 1, 0 < \phi_p^b < 1 \end{aligned} \quad (11)$$

The reduced volume fractions of the α and β phases, denoted as v^α and v^β , respectively, satisfy the constraint $v^\alpha + v^\beta = 1$. We note that the method developed by Mester, Lynd, and Fredrickson^[42] is essentially rooted in this optimization perspective. Importantly, the above formulation allows for computing both the GCE free energy \tilde{F}_g and the GE free energy G purely from the CE free energy \tilde{F} without requiring any additional computations in their respective ensembles.

ANALYTICAL MODELS

In rare scenarios, free energies and chemical potentials have analytical expressions. Our formulation can be straightforwardly applied to such cases. As an illustrative example, we consider disordered phases (DIS) in a binary blend of two types of block copolymers, each consisting of any number of A and/or B blocks, which generalizes the simple A/B binary blend. According to the Flory-Huggins theory, the CE free energy density of a DIS phase in this binary blend is given by,^[35]

$$\tilde{F} = \frac{\phi_1}{\alpha_1} \ln \phi_1 + \frac{\phi_2}{\alpha_2} \ln \phi_2 + \chi N \phi_A \phi_B \quad (12)$$

Here, $\alpha_1 N$ and $\alpha_2 N$ are the number of segments in block copolymer 1 and 2, respectively. The Flory-Huggins interaction parameter χ characterizes the immiscibility between A and B segments. ϕ_1 and ϕ_2 represent the respective volume fractions of block copolymers 1 and 2, while $\phi_A = f_1 \phi_1 + f_2 \phi_2$ and $\phi_B = (1 - f_1) \phi_1 + (1 - f_2) \phi_2$ are respective volume fractions of A and B segments with f_1 and f_2 being respective volume fractions of A segments in block copolymers 1 and 2.

To compute the effective chemical potential, we select block copolymer 2 as the reference component ($\tilde{\mu}_2 = 0$). Thus, only $\tilde{\mu}_1$ is relevant. Using Eq. (4), the intermediate quantities γ_1 and γ_2 are derived as:

$$\gamma_1 = \frac{1}{\alpha_1} + \frac{1}{\alpha_1} \ln \phi_1 + \chi N \{ 2f_1(1-f_1)\phi_1 + [f_1(1-f_2) + f_2(1-f_1)]\phi_2 \} \quad (13)$$

$$\gamma_2 = \frac{1}{\alpha_2} + \frac{1}{\alpha_2} \ln \phi_2 + \chi N \{ 2f_2(1-f_2)\phi_2 + [f_1(1-f_2) + f_2(1-f_1)]\phi_1 \} \quad (14)$$

The effective chemical potential $\tilde{\mu}_1$ is then obtained by subtracting γ_2 from γ_1 :

$$\begin{aligned} \tilde{\mu}_1 = \frac{1}{\alpha_1} \ln \phi_1 - \frac{1}{\alpha_2} \ln(1 - \phi_1) + \chi N \phi_1 (4f_1 f_2 - 2f_1^2 - 2f_2^2) + \\ \chi N (f_1 - f_2 - 2f_1 f_2 + 2f_2^2) + \frac{1}{\alpha_1} - \frac{1}{\alpha_2} \end{aligned} \quad (15)$$

As can be seen, the introduction of γ_p significantly simplifies the derivation of effective chemical potentials. For example, computing γ_1 only involves terms containing ϕ_1 explicitly, bypassing the derivatives of composite functions imposed by the mass conservation constraint. This advantage becomes increasingly pronounced as either the number of components or the number of species increases.

For a binary system, two-phase equilibrium conditions can be obtained from Eq. (7),

$$\begin{cases} \tilde{\mu}_1^a(\phi_1^a) = \tilde{\mu}_1^b(\phi_1^b) \\ \tilde{\mu}_1^a(\phi_1^a) = \frac{\tilde{F}^a(\phi_1^a) - \tilde{F}^b(\phi_1^b)}{\phi_1^a - \phi_1^b} \end{cases} \quad (16)$$

Fig. 1 depicts the free energy curve for A-rich DIS phase and B-rich DIS phase in a binary blend of AB diblock copolymers (component 1) and AB₃ miktoarm block copolymers (component 2). The double-well structure observed in the free energy curve is typical for two-phase coexistence. We treat the phase equilibrium condition given by Eq. (16) as a set of nonlinear equations. By solving these equations we can obtain the two-phase coexistence points, which appear in Fig. 1 as two common tangent points.

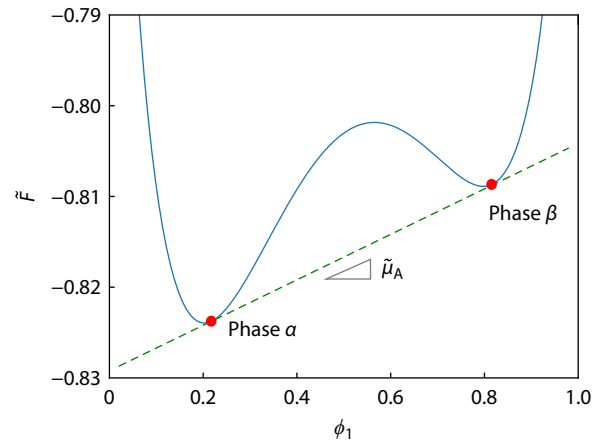


Fig. 1 Free energy (\tilde{F}) as a function of the volume fraction (ϕ_1) for disordered phases with $\chi N = 3.3$, $\alpha_1 = 1.0$, $\alpha_2 = 1.2$, $f_1 = 0.9$, $f_2 = 0.1$ in the AB/AB₃ binary blend. The dashed line is the common tangent line of the free energy curve where two common tangent points denoted as solid disks are phase coexistence points.

Another common method^[41] for finding the phase coexistence points involves converting the CE free energy into GCE free energy. In practice, we first evaluate free energies in CE and then utilize Eq. (8) to convert them to the GCE free energies. The equilibrium condition is given by Eq. (9) as,

$$\tilde{F}_g^a(\phi_1^a) = \tilde{F}_g^b(\phi_1^b) \quad (17)$$

As shown in Fig. 2(a), the intersection of GCE curves marks the phase coexistence from which the effective potential at phase equilibrium is obtained. According to Eq. (6), the corresponding volume fractions are derived by inverting the function $\tilde{\mu}_1(\phi_1)$, as shown in Fig. 2(b). Note that the function $\tilde{\mu}_1(\phi_1)$ is explicit while its inverse $\phi_1(\tilde{\mu}_1)$ is implicit. It is also worth noting that, while in principle $\tilde{\mu}_1$ is unbounded, the volume fractions remain confined between 0 and 1. Thus it is more intuitive and convenient to perform calculations in CE rather than in GCE.

NUMERICAL MODELS

We demonstrate that our effective chemical potential formulation can still be applied explicitly when free energies and related quantities are only available through numerical computations. Here we use self-consistent field theory (SCFT) calculations as an example. Consider an incompressible polymer blend consisting of n_c block copolymer components in a volume V , the free energy in CE at the mean-field level is given by:^[34,47]

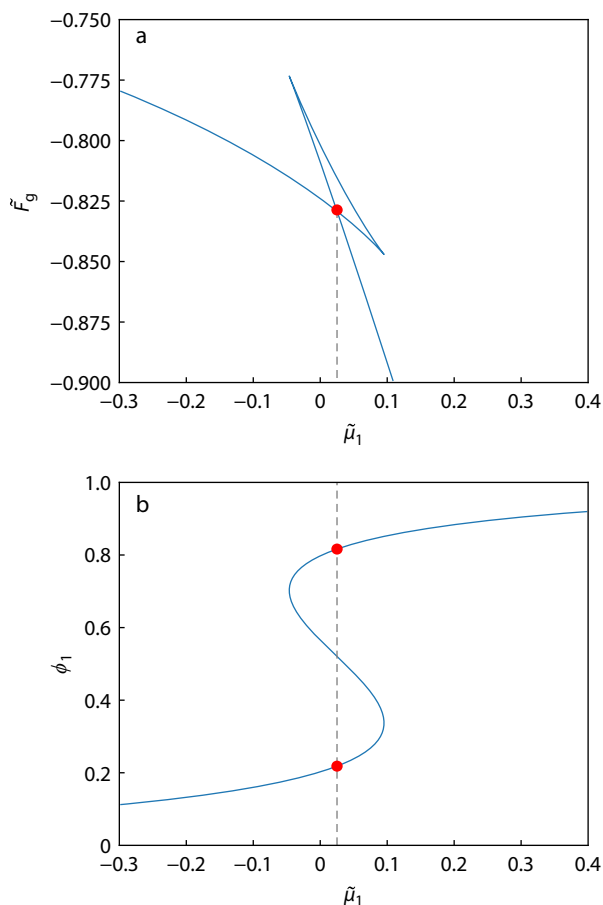


Fig. 2 (a) The grand canonical free energy (\tilde{F}_g) and (b) the volume fraction of (ϕ_1) for the disorder phase as a function of the effective chemical potential ($\tilde{\mu}_1$). The intersection in the upper panel indicates phase coexistence. The volume fractions of ($\tilde{\mu}_1$) at the phase coexistence are found as the intersections of the dashed line and the curve.

$$\tilde{F} = \frac{1}{2} \sum_{i=1}^{n_s} \sum_{j=1}^{n_s} \frac{1}{V} \int d\mathbf{r} \chi_{ij} N \phi_{si}(\mathbf{r}) \phi_{sj}(\mathbf{r}) - \sum_{i=1}^{n_s} \frac{1}{V} \int d\mathbf{r} w_i(\mathbf{r}) \phi_{si}(\mathbf{r}) - \sum_{p=1}^{n_c} \frac{\phi_p}{\alpha_p} \ln Q_p + \sum_{p=1}^{n_c} \frac{\phi_p}{\alpha_p} \left(\ln \frac{\phi_p}{\alpha_p} - 1 \right) \tag{18}$$

where $\phi_{si}(\mathbf{r})$ represents the equilibrium density field of each species (*i.e.* the type of segment) with $i \in \{1, 2, \dots, n_s\}$, ϕ_p is the volume fraction of each component in the system with $p \in \{1, 2, \dots, n_c\}$, and n_s and n_c are the number of species and the number of components, respectively. The auxiliary fields conjugated to the density fields are denoted as w_i . The normalized chain length of each component is $\alpha_p = N_p/N$ with N being an arbitrary chosen reference chain length. For each component p , Q_p represents its dimensionless single-chain partition function following the formulation in Ref.^[47] SCFT is the state-of-the-art numerical technique for calculating the free energy as well as Q_p .^[48–50]

By noting that $\phi_{si}(\mathbf{r})$ is independent of ϕ_p , deriving γ_p from Eq. (18) is similar to the previous section,

$$\gamma_p = \frac{1}{\alpha_p} \ln \frac{\phi_p}{\alpha_p} - \frac{1}{\alpha_p} \ln Q_p \tag{19}$$

Using Eq. (3), we can readily obtain the effective chemical potential of any component p by choosing one of components (r) as the reference,

$$\tilde{\mu}_p = \frac{1}{\alpha_p} \ln \frac{\phi_p}{\alpha_p Q_p} - \frac{1}{\alpha_r} \ln \frac{\phi_r}{\alpha_r Q_r} \tag{20}$$

This equation is equivalent to Eq. (47) of Ref. [41], confirming the validity of our formulation. Moreover, our approach clarifies that the notation “ μ ” in their work should refer to the effective chemical potential rather than the bare chemical potential.

Obviously, both the free energies in Eq. (18) and the effective chemical potentials in Eq. (20) can be obtained *via* SCFT calculations in CE (CE-SCFT). Consequently, as demonstrated in the previous section, the solution of phase coexistence can be carried out without performing further SCFT calculations in other ensembles. In the following section, we will demonstrate how to compute phase coexistence of two ordered phases in both binary and ternary blends of block copolymers using CE-SCFT based on our formulation.

Binary AB/BC Blends

An AB/BC diblock copolymer blend with $f_A = f_C = 0.357$, $\chi_{AB}N = \chi_{BC}N = 20$ and $\chi_{AC}N = 35$ is intentionally chosen to be the same as that in Ref. [43] for the convenience of validating our results. According to Ref. [43], such a blend exhibits coexistence of several ordered phases, including the alternating double gyroid (G^A) and hexagonal-packed alternating cylinders with A majority cylinders (C_{6a}^A). We reproduce the free energy curves of both phases as a function of ϕ_{AB} using CE-SCFT as shown in Fig. 3. Then, by solving the nonlinear system of equations in Eq. (7), we obtain the corresponding phase equilibrium solution, which is depicted in Fig. 3 as the common tangent line —analogous to that shown in Fig. 1.

Similar to Fig. 2, using our formulation it is also possible to determine phase coexistence in GCE by converting the calculated CE free energies to the GCE free energies using Eq. (8) without performing GCE-SCFT. Fig. 4(a) illustrates the intersection of two GCE free energy curves, allowing us to determine the $\tilde{\mu}_{AB}$ at phase coexistence. The corresponding volume fractions of the two coexistence phases are then obtained by looking up the mapping between $\tilde{\mu}_{AB}$ and ϕ_{AB} given by Eq. (20), as shown in Fig. 4(b).

Ternary AB/BC/ABC Blends

Our formulation can be straightforwardly extended to three-component systems. By adding an additional linear triblock terpolymer ABC to the previous AB/BC blend, we obtain a ternary AB/BC/ABC blend. To be consistent with Ref. [43], we also consider a blend with volume fractions of A and C blocks in ABC being $f'_A = f'_C = 0.319$ and its number of segments $N' = 1.3428N$. Other parameters remain the same as in the previous AB/BC blend. By setting the ABC component as the reference, CE-SCFT calculations result in a series of CE free energies as well as $\tilde{\mu}_{AB}^\varphi$ and $\tilde{\mu}_{BC}^\varphi$ ($\varphi = G^A, C_{6a}^A, \text{AB-richG}$) by varying ϕ_{AB} and ϕ_{BC} as shown in Fig. 5(a). In a ternary system, the three-phase equilibrium ($G^A, C_{6a}^A, \text{AB-richG}$) can be determined by constructing a common tangent plane, which is equivalent to pairwise coexistence between the three ordered phases, involving three common tangent lines. The resulting phase coexistence points and

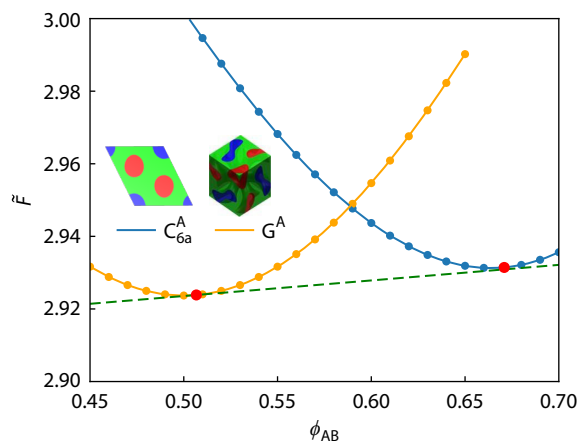


Fig. 3 Free energy (\bar{F}) per diblock chain as a function of AB diblock volume fraction ϕ_{AB} for alternating double gyroid (G^A) and hexagonal packed alternating cylinders with A majority cylinders (C_{6a}^A) phases. The dashed line is the common tangent line indicating phase equilibrium. The solid points are the common tangent points.

the enclosed three-phase region are shown in Fig. 5(b). According to Eq. (7), the three tangent points satisfy the condition that their effective chemical potentials, $\tilde{\mu}_{AB}^k$ and $\tilde{\mu}_{BC}^k$, are equal to each other, respectively, and also equal to the slopes of the respective common tangent lines. The common tangent plane construction helps to elucidate the concept of phase equilibrium in a more intuitive way, which offers a consistent understanding of the physical meaning of the effective chemical potential and emphasizes the practical significance of our formulation.

From the theoretical perspective of effective chemical potential, we reveal that the numerical solutions to phase equilibrium problems in GCE, semi-GCE, and GE can all be unified and solved within the CE. By solving CE-SCFT, the thermodynamic variables obtained can be directly mapped to other ensembles without the need to reconstruct the SCFT equations for specific ensembles. The following comparative analysis of the traditional implementation paths for GCE, semi-GCE, and GE demonstrates the implicit relationship between the control variables of these ensembles and the effective chemical potential in the canonical ensemble.

Grand Canonical Ensemble

Park, Bates and Dorfman investigated ternary blends by identifying the phase boundaries of candidate phases within GCE.^[43] They used the chemical potentials, μ_k , as input parameters and volume fractions, ϕ_k , were computed from them by using the

relation $\phi_k = e^{\frac{\mu_k}{k_B T}} Q_k$, where Q_k represents the single-chain partition function for component k . Subsequently, they implemented a GCE-SCFT and performed calculations in GCE. However, it appears that they did not realize that in their formulation the input parameters, μ_k in GCE, actually represent "effective chemical potentials" because they have set the chemical potential of one component to 0. This subtle distinction has been addressed by our formulation which clearly distinguished bare chemical potentials and effective chemical potentials, avoiding any confusion and misunderstandings. In our approach, effective chemical potentials can be directly obtained from CE-SCFT

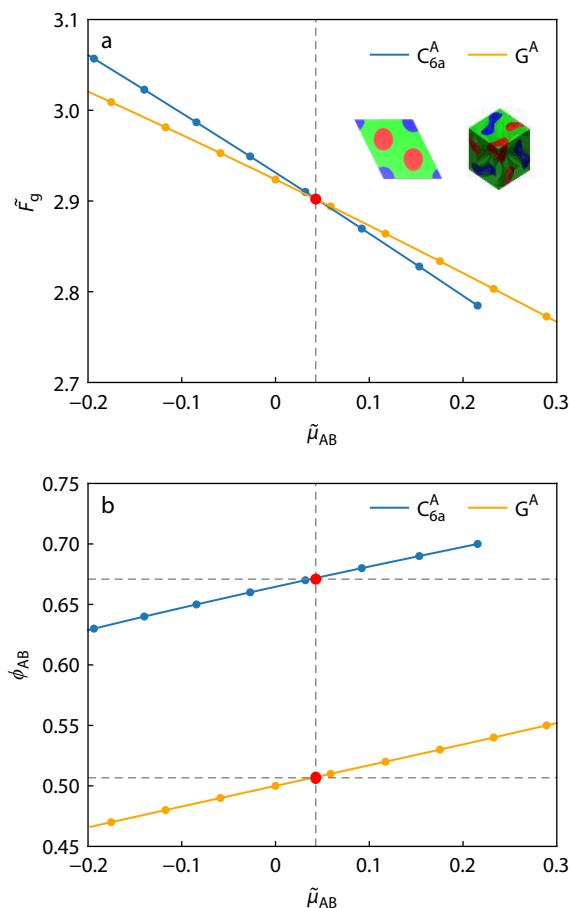


Fig. 4 (a) The grand free energy (\bar{F}_g) and (b) the volume fraction of AB for each phase as a function of the effective chemical potential ($\tilde{\mu}_{AB}$). The dashed line in (a) indicates phase equilibrium, while the dashed lines in (b) represent the volume fractions of AB at phase equilibrium.

according to Eq. (20), allowing us to seamlessly convert the CE free energy into the GCE free energy without performing any GCE-SCFT simulations as demonstrated in the previous section and in Fig. 5.

Semigrand Canonical Ensemble

Xie and Shi^[44] developed a method that implements the SCFT within the so-called semigrand canonical ensemble (semi-GCE) to streamline the analysis of phase behavior of AB/C/D ternary blends. They set μ_1 (the chemical potential of the AB copolymers) to 0 by invoking the incompressibility condition, which is equivalent to our approach of designating the AB component as the reference. Therefore, the two remaining chemical potentials for C (μ') and D (μ'') components are, in fact, effective chemical potentials in our formulation. μ is then transformed to the average concentration of D homopolymers, ϕ_3 , according to $\phi_3 = \gamma_D e^{\frac{\mu}{k_B T}} Q_3$, where Q_3 is the single chain partition function of component D. Consequently, the free energy in semi-GCE, $\Phi_{SG}(\mu', \phi_3)$, treats μ' and ϕ_3 as its independent variables. The form of the SCFT equations is similar to that in GCE, except for the equation used to calculate $\phi_D(\mathbf{r})$. In this way, it addresses some of the aforementioned disadvantages, namely that ϕ_3 is typically bounded between 0 and 1, making it a more manage-

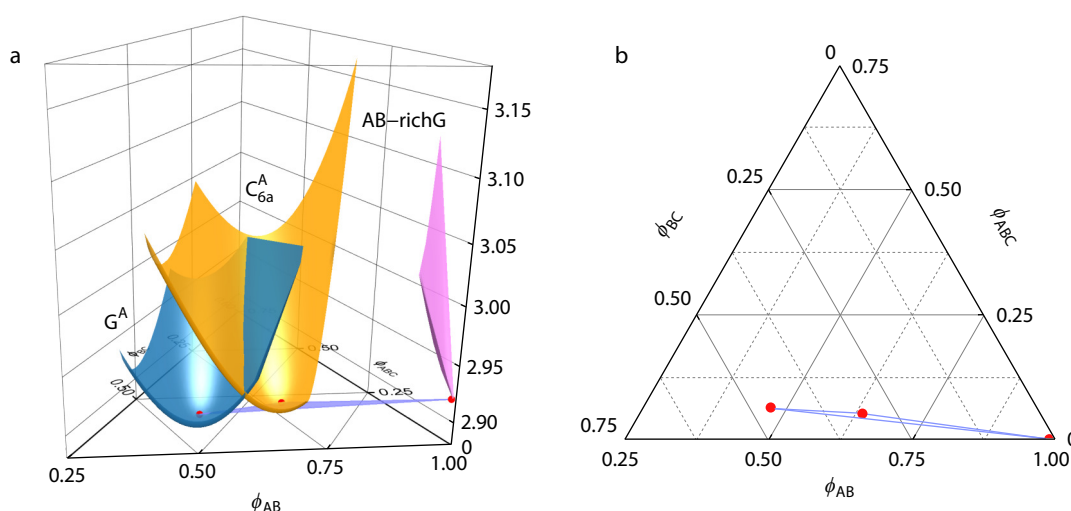


Fig. 5 (a) Free energy surfaces of G^A , C_{6a}^A and AB-richG phases as a function of volume fractions. The common tangent plane highlights the three-phase coexistence region with three vertices corresponding to three coexistence phases. (b) The projected ternary phase diagram illustrates the three-phase coexistence region in 2D. The boundary points correspond to the common tangent points on the free energy surfaces shown in (a).

able and intuitive variable as compared to μ , which can theoretically range from negative to positive infinity. However, it should be noted that this approach also requires reformulating CE-SCFT and consequently, additional semi-GCE SCFT software has to be implemented.

Gibbs Ensemble

To avoid numerical instability caused by poor initial values when solving GCE-SCFT, Mester, Lynd, and Fredrickson^[42] proposed a method that optimizes the free energy directly within the Gibbs ensemble (GE) which takes volume fractions as independent variables. They considered a binary blend of A/AB, where the GE free energy of overall system is expressed as $G = V_I \tilde{F}_I + V_{II} \tilde{F}_{II}$. The polymers are distributed between two simulation cells with volumes $V_I = \frac{\phi_0 - \phi_2}{\phi_1 - \phi_2}$ and $V_{II} = \frac{\phi_1 - \phi_0}{\phi_1 - \phi_2}$, where ϕ_1 and ϕ_2 rep-

resent the volume fractions of the two possible coexisting phases, respectively, and ϕ_0 is an appropriately chosen initial volume fraction. At the two-phase coexistence point, the GE free energy reaches its minimum value. In their method, G is computed directly from GE-SCFT which differs from CE-SCFT. Thus, it also requires implementation of a GE-SCFT solver rather than using existing CE-SCFT solvers. Our method, however, can readily transform thermodynamic quantities from CE to GE which avoids performing GE-SCFT calculations, thereby enhancing its versatility and efficiency.

In summary, all of the aforementioned methods deeply integrate the solution of phase equilibria into a customized self-consistent field method in a particular ensemble, which requires additional adjustments for each specific ternary blend system. The coupling results in a more complex and less transparent formulation that may limit the generalizability of their methods. Additionally, their methods are primarily designed to solve phase equilibria in ternary component systems, which restricts their applicability to more complex component systems. In contrast, our method does not couple SCFT with the solution of phase equilibria, making it simpler

and more intuitive. As our approach does not make a priori assumption about the number of components, it can be extended to accommodate systems with more components, making it easier to apply and extend to a wider range of scenarios.

CONCLUSIONS

In this study, we introduce the concept of the “effective chemical potential” and develop a unified framework for solving phase equilibria in multi-component polymer blend systems. This framework establishes universal relationships among thermodynamic quantities in the canonical ensemble, grand canonical ensemble, semi-grand canonical ensemble, and Gibbs ensemble, achieving a theoretical unification for cross-ensemble phase coexistence determination. The core contribution of this method lies in the fact that it eliminates the need to reconstruct the self-consistent field theory (SCFT) calculation framework for different ensembles. Instead, it directly utilizes the SCFT results from the canonical ensemble, allowing for the flexible conversion between ensembles and facilitating the analysis of system phase behavior.

Building on this concept, various backend methods for solving phase equilibrium can be flexibly selected, significantly reducing the computational complexity typically associated with multi-component phase equilibrium calculations. The introduction of y_p enables efficient calculations of effective chemical potentials, resulting in a more transparent formulation. Moreover, our concept enables better utilization of CE-SCFT calculation results and offers potential optimization opportunities for developing highly efficient numerical methods. We validated the robustness and versatility of our framework by applying it to both analytical models based on Flory-Huggins theory and numerical models derived from CE-SCFT calculations. The application of our method to binary (AB/BC) and ternary (AB/BC/ABC) blends of block copolymers demonstrated its ability to reproduce known results in a more con-

sistent manner.

The core advantage of our framework lies in its general applicability across various types of systems, independent of specific theoretical models for phase equilibrium. This flexibility not only allows seamless integration of well-known theoretical models, such as Flory-Huggins theory and SCFT, but also opens avenues for exploring new theoretical models in the future. We expect it to become a valuable tool for studying the phase behavior of multi-component polymer blends, facilitating the exploration of phase behaviors in more complex blend systems with additional parameters.

Conflict of Interests

The authors declare no interest conflict.

Electronic Supplementary Information

Electronic supplementary information (ESI) is available free of charge in the online version of this article at <http://doi.org/10.1007/s10118-025-3369-8>.

ACKNOWLEDGMENTS

This work was financially supported by the National Natural Science Foundation of China (No. 21873021).

REFERENCES

- Clarke, R. W.; Sandmeier, T.; Franklin, K. A.; Reich, D.; Zhang, X.; Vengallur, N.; Patra, T. K.; Tannenbaum, R. J.; Adhikari, S.; Kumar, S. K.; Rovis, T.; Chen, E. Y. X. Dynamic crosslinking compatibilizes immiscible mixed plastics. *Nature* **2023**, *616*, 731–739.
- Gdowski, Z. M.; Swartzendruber, S. M.; Mahanthappa, M. K.; Bates, F. S. Diblock copolymer blends do not mimic metal alloys. *Macromolecules* **2024**, *57*, DOI: 10.1021/acs.macromol.4c01146.
- Coughlin, M. L.; Huang, D. E.; Edgar, C. M.; Kotula, A. P.; Migler, K. B. Composition dependence of flow-induced crystallization in high-density polyethylene/isotactic polypropylene blends. *Macromolecules* **2024**, *57*, 9751–9765.
- Wang, Y.; Li, G.; Zhu, H.; Wan, Z.; Zhang, X.; Ma, Y.; Xie, L. Morphological evolution and structural orientation of poly(ϵ -caprolactone)/poly(lactic acid) biodegradable blend films under complex coupling flow. *Macromolecules* **2024**, *57*, 4345–4356.
- Wang, Q.; Yu, X.; Chen, X.; Gao, J.; Shi, D.; Shen, Y.; Tang, J.; He, J.; Li, A.; Yu, L.; Ding, J. A facile composite strategy to prepare a biodegradable polymer based radiopaque raw material for “visualizable” biomedical implants. *ACS Appl. Mater. Interfaces* **2022**, *14*, 24197–24212.
- Li, Q.; Woo, D.; Kim, J. K.; Li, W. Truly “Inverted” cylinders and spheres formed in the A(AB)₃/AC blends of B/C hydrogen bonding interactions. *Macromolecules* **2022**, *55*, 6525–6535.
- Li, W.; Duan, C.; Shi, A. C. Nonclassical spherical packing phases self-assembled from AB-type block copolymers. *ACS Macro Lett.* **2017**, *6*, 1257–1262.
- He, W.; Wang, F.; Qiang, Y.; Pan, Y.; Li, W.; Liu, M. Asymmetric binary spherical phases self-assembled by mixing AB diblock/abc triblock copolymers. *Macromolecules* **2023**, *56*, 719–729.
- Chen, J.; Rong, C.; Lin, T.; Chen, Y.; Wu, J.; You, J.; Wang, H.; Li, Y. Stable co-continuous PLA/PBAT blends compatibilized by interfacial stereocomplex crystallites: toward full biodegradable polymer blends with simultaneously enhanced mechanical properties and crystallization rates. *Macromolecules* **2021**, *54*, 2852–2861.
- Hassan, M.; Mohanty, A. K.; Misra, M. Additive manufacturing of a super toughened biodegradable polymer blend: structure-property-processing correlation and 3D printed prosthetic part development. *ACS Appl. Polym. Mater.* **2024**, *6*, 3849–3863.
- Maiti, M.; Jasra, R. V.; Kusum, S. K.; Chaki, T. K. microcellular foam from ethylene vinyl acetate/polybutadiene rubber (EVA/BR) based thermoplastic elastomers for footwear applications. *Indus. Eng. Chem. Res.* **2012**, *51*, 10607–10612.
- Peng, B.; Yang, Y.; Ju, T.; Cavicchi, K. A. Fused Filament Fabrication 4D printing of a highly extensible, self-healing, shape memory elastomer based on thermoplastic polymer blends. *ACS Appl. Mater. Interfaces* **2020**, *13*, 12777–12788.
- Liu, Y. X.; Delaney, K. T.; Fredrickson, G. H. Field-Theoretic simulations of fluctuation-stabilized aperiodic “bricks-and-Mortar” mesophase in miktoarm star block copolymer/homopolymer blends. *Macromolecules* **2017**, *50*, 6263–6272.
- Riera-Galindo, S.; Leonardi, F.; Pfattner, R.; Mas-Torrent, M. Organic semiconductor/polymer blend films for organic field-effect transistors. *Adv. Mater. Technol.* **2019**, *4*, 1900104.
- Kang, J.; Shin, N.; Jang, Y. P.; Prabhu, V. M.; Yoon, D. Y. Structure and properties of small molecule-polymer blend semiconductors for organic thin film transistors. *J. Am. Chem. Soc.* **2008**, *130*, 12273–12275.
- Alshammari, A. H.; Alshammari, M.; Ibrahim, M.; Alshammari, K. Taha new hybrid PVC/PVP polymer blend modified with Er₂O₃ nanoparticles for optoelectronic applications. *Polymers* **2023**, *15*, 684–684.
- Jiang, L.; Yang, L.; Yuan, Y.; Zhu, Q.; Wu, W.; Wang, X.; Xu, W.; Qiu, L. Flexible optoelectronic synapses based on conjugated polymer blends for ultra broadband spectrum light perception. *ACS Mater. Lett.* **2024**, *6*, 1606–1615.
- Pucci, A.; Bizzarri, R.; Ruggeri, G. Polymer composites with smart optical properties. *Soft Matter* **2011**, *7*, 3689.
- Guo, X.; Liu, L.; Zhuang, Z.; Chen, X.; Ni, M.; Li, Y.; Cui, Y.; Zhan, P.; Yuan, C.; Ge, H.; Wang, Z.; Chen, Y. A new strategy of lithography based on phase separation of polymer blends. *Scientific Reports* **2015**, *5*, DOI: 10.1038/srep15947.
- Huang, C. Z.; Moosmann, M.; Jin, J.; Heiler, T.; Walheim, S.; Schimmel, T. Polymer blend lithography: a versatile method to fabricate nanopatterned selfassembled monolayers. *Beilstein J. Nanotechnol.* **2012**, *3*, 620–628.
- Robeson, L. M. Applications of polymer blends: emphasis on recent advances. *Polym. Eng. Sci.* **1984**, *24*, 587–597.
- Imre, B.; Pukánszky, B. Compatibilization in bio-based and biodegradable polymer blends. *Eur. Polym. J.* **2013**, *49*, 1215–1233.
- Okuzono, T.; Ozawa, K.; Doi, M. Simple model of skin formation caused by solvent evaporation in polymer solutions. *Phys. Rev. Lett.* **2006**, *97*, 136103.
- Zhou, J.; Jiang, Y.; Doi, M. Cross interaction drives stratification in drying film of binary colloidal mixtures. *Phys. Rev. Lett.* **2017**, *118*, 108002.
- Buxton, G. A.; Clarke, N. Ordering polymer blend morphologies via solvent evaporation. *Europhysics Letters (EPL)* **2007**, *78*, 56006.
- Wodo, O.; Ganapathysubramanian, B. Modeling morphology evolution during solventbased fabrication of organic solar cells. *Comput. Mater. Sci.* **2012**, *55*, 113–126.
- Zheng, C.; Zhang, B.; Bates, F. S.; Lodge, T. P. Effect of poly[oligo(ethylene glycol) methyl ether methacrylate] side chain length on the brush swelling behavior in A/B/A-B ternary

- blends with polystyrene. *Soft Matter* **2023**, *19*, 4519–4525.
- 28 Xie, S.; Zhang, B.; Bates, F. S.; Lodge, T. P. Phase behavior of salt-doped A/B/AB ternary polymer blends: the role of homopolymer distribution. *Macromolecules* **2021**, *54*, 6990–7002.
- 29 Zhao, M.; Li, W. Laves phases formed in the binary blend of AB₄ miktoarm star copolymer and A-homopolymer. *Macromolecules* **2019**, *52*, 1832–1842.
- 30 Zhao, F.; Dong, Q.; Li, Q.; Liu, M.; Li, W. Emergence and stability of exotic “binary” HCP-type Spherical phase in binary AB/AB blends. *Macromolecules* **2022**, *55*, 10005–10013.
- 31 Xie, J.; Shi, A. C. Formation of complex spherical packing phases in diblock copolymer/homopolymer blends. *Giant* **2021**, *5*, 100043.
- 32 Bates, F. S.; Fredrickson, G. H. Block copolymers—designer soft materials. *Phys. Today* **1999**, *52*, 32–38.
- 33 Boles, M. A.; Engel, M.; Talapin, D. V. Self-Assembly of colloidal nanocrystals: from intricate structures to functional materials. *Chem. Rev.* **2016**, *116*, 11220–11289.
- 34 Fredrickson, G. H. *The Equilibrium Theory of Inhomogeneous Polymers*; Oxford University Press, **2006**.
- 35 Rubinstein, M.; Colby, R. H. *Polymer physics*; Oxford University Press, **2003**.
- 36 Mao, S.; Kuldinow, D.; Haataja, M. P.; Košmrlj, A. Phase behavior and morphology of multicomponent liquid mixtures. *Soft Matter* **2019**, *15*, 1297–1311.
- 37 Janert, P. K.; Schick, M. Phase behavior of ternary homopolymer/diblock blends: microphase unbinding in the symmetric system. *Macromolecules* **1997**, *30*, 3916–3920.
- 38 Huang, C.; Cruz, M. O. d. I.; Swift, B. W. Phase separation of ternary mixtures: symmetric polymer blends. *Macromolecules* **1995**, *28*, 7996–8005.
- 39 Yadav, M.; Bates, F. S.; Morse, D. C. Effects of segment length asymmetry in ternary diblock co-polymer–homopolymer mixtures. *Macromolecules* **2019**, *52*, 4091–4102.
- 40 Matsen, M. W. Stabilizing new morphologies by blending homopolymer with block copolymer. *Phys. Rev. Lett.* **1995**, *74*, 4225–4228.
- 41 Matsen, M. W. New Fast SCFT algorithm applied to binary diblock copolymer/homopolymer blends. *Macromolecules* **2003**, *36*, 9647–9657.
- 42 Mester, Z.; Lynd, N. A.; Fredrickson, G. H. Numerical self-consistent field theory of multicomponent polymer blends in the Gibbs ensemble. *Soft Matter* **2013**, *9*, 11288.
- 43 Park, S. J.; Bates, F. S.; Dorfman, K. D. Alternating Gyroid in Block Polymer Blends. *ACS Macro Lett.* **2022**, *11*, 643–650.
- 44 Xie, J.; Shi, A. C. Theory of complex spherical packing phases in Diblock copolymer/homopolymer blends. *Macromolecules* **2023**, *56*, 10296–10312.
- 45 Hong, K. M.; Noolandi, J. Theory of inhomogeneous multicomponent polymer systems. *Macromolecules* **1981**, *14*, 727–736.
- 46 Legendre, A. M. *Mémoire sur l'intégration de quelques équations aux différences partielles*; Imprimerie royale, **1787**; pp 309–351.
- 47 Zhang, Y.; Huang, W.; Liu, Y. X. Automated chain architecture screening for discovery of block copolymer assembly with graph enhanced self-consistent field theory. *Commun. Mater.* **2024**, *5*, 266.
- 48 Guo, Z.; Zhang, G.; Qiu, F.; Zhang, H.; Yang, Y.; Shi, A. C. Discovering ordered phases of block copolymers: new results from a generic fourier-space approach. *Phys. Rev. Lett.* **2008**, *101*, 028301.
- 49 Xu, W.; Jiang, K.; Zhang, P.; Shi, A. C. A strategy to explore stable and metastable ordered phases of block copolymers. *J. Phys. Chem. B* **2013**, *117*, 5296–5305.
- 50 Arora, A.; Morse, D. C.; Bates, F. S.; Dorfman, K. D. Accelerating self-consistent field theory of block polymers in a variable unit cell. *J. Chem. Phys.* **2017**, *146*, 244902.